

# UC Irvine

## UC Irvine Previously Published Works

### Title

A novel sensitive assay for detection of a biomarker of pericyte injury in cerebrospinal fluid

### Permalink

<https://escholarship.org/uc/item/81x9m1k3>

### Journal

Alzheimer's & Dementia, 16(6)

### ISSN

1552-5260

### Authors

Sweeney, Melanie D  
Sagare, Abhay P  
Pachicano, Maricarmen  
[et al.](#)

### Publication Date

2020-06-01

### DOI

10.1002/alz.12061

Peer reviewed



Published in final edited form as:

*Alzheimers Dement.* 2020 June ; 16(6): 821–830. doi:10.1002/alz.12061.

## A novel sensitive assay for detection of a biomarker of pericyte injury in cerebrospinal fluid

Melanie D. Sweeney<sup>1,\*</sup>, Abhay P. Sagare<sup>1,\*</sup>, Maricarmen Pachicano<sup>1</sup>, Michael G. Harrington<sup>2</sup>, Elizabeth Joe<sup>3,4</sup>, Helena C. Chui<sup>3,4</sup>, Lon S. Schneider<sup>3,4,5</sup>, Axel Montagne<sup>1</sup>, John M. Ringman<sup>3,4</sup>, Anne M. Fagan<sup>6,7,8</sup>, John C. Morris<sup>6,8</sup>, Judy Pa<sup>3,9</sup>, Daniel A. Nation<sup>1,3,10</sup>, Arthur W. Toga<sup>3,9</sup>, Berislav V. Zlokovic<sup>1,3,†</sup>

<sup>1</sup>Department of Physiology and Neuroscience, Zilkha Neurogenetic Institute, Keck School of Medicine, University of Southern California, Los Angeles, CA, USA

<sup>2</sup>Huntington Medical Research Institutes, Pasadena, CA, USA

<sup>3</sup>Alzheimer's Disease Research Center, Keck School of Medicine, University of Southern California, Los Angeles, CA, USA

<sup>4</sup>Department of Neurology, Keck School of Medicine, University of Southern California, Los Angeles, CA, USA

<sup>5</sup>Department of Psychiatry and Behavioral Sciences, University of Southern California, Los Angeles, CA, USA

<sup>6</sup>Department of Neurology, Washington University School of Medicine, St. Louis, MO, USA

<sup>7</sup>The Hope Center for Neurodegenerative Disorders, Washington University School of Medicine, St. Louis, MO, USA

<sup>8</sup>The Knight Alzheimer's Disease Research Center, Washington University School of Medicine, St. Louis, MO, USA

<sup>9</sup>Laboratory of Neuro Imaging (LONI), USC Stevens Neuroimaging and Informatics Institute, Keck School of Medicine, University of Southern California, Los Angeles, CA, USA

<sup>10</sup>Department of Psychology, University of Southern California, Los Angeles, CA, USA

### Abstract

**INTRODUCTION:** Blood-brain barrier breakdown and loss of brain capillary pericytes contributes to cognitive impairment. Pericytes express platelet-derived growth factor receptor- $\beta$  (PDGFR $\beta$ ) that regulates brain angiogenesis and blood vessel stability. Elevated soluble PDGFR $\beta$  (sPDGFR $\beta$ ) levels in cerebrospinal fluid (CSF) indicate pericyte injury and BBB breakdown, which is an early biomarker of human cognitive dysfunction.

<sup>†</sup>Address correspondence: Berislav V. Zlokovic, M.D., Ph.D., Zilkha Neurogenetic Institute, 1501 San Pablo Street, Los Angeles, CA 90089, Phone: 323.442.2722 / Fax: 323.666.2184, zlokovic@usc.edu.

\*Equally contributed first co-authors

**METHODS:** A combination of reagents and conditions were tested, optimized, and validated on the Meso Scale Discovery electrochemiluminescence platform to develop a new sPDGFR $\beta$  immunoassay that was used to measure sPDGFR $\beta$  in human CSF from 147 individuals.

**RESULTS:** We developed standard operating procedures for a highly sensitive and reproducible sPDGFR $\beta$  immunoassay with a dynamic range from 100–26,000 pg/mL, and confirmed elevated CSF sPDGFR $\beta$  levels in individuals with cognitive dysfunction.

**DISCUSSION:** This assay could be applied at different laboratories to study brain pericytes and microvascular damage in relation to cognition in disorders associated with neurovascular and cognitive dysfunction.

### Keywords

Pericytes; vascular; blood-brain barrier; biomarker; cerebrospinal fluid; cognitive impairment

## 1. INTRODUCTION

Proper functioning of the central nervous system (CNS) requires highly coordinated actions of the neurovascular unit, which comprises vascular cells, glia, and neurons [1–4]. Increasing evidence supports that neurovascular dysfunction contributes to complex neurodegenerative disorders, including Alzheimer’s disease (AD) [2,3,5–10]. Human neuroimaging and biofluid studies have shown this during different stages of AD pathophysiology, as well as in a neuropathological analysis of AD brains. Multiple studies of AD brains reveal blood-brain barrier (BBB) breakdown with the accumulation of several blood-derived proteins in brain tissue [11–17] and degeneration of brain capillary pericytes [16–19] that is accelerated by the apolipoprotein E (*APOE*)  $\epsilon$ 4 allele [11,12,15,17,20,21], the major genetic risk factor for sporadic AD.

Pericytes and vascular smooth muscle cells (SMCs) are vascular mural cells that cover most of the endothelium of brain capillaries, and arterioles and arteries, respectively, forming the outer layer of brain vessels [1,6,22]. Cell signaling between endothelial-secreted platelet-derived growth factor (PDGF)-BB and PDGF receptor- $\beta$  (PDGFR $\beta$ ) on pericytes and SMCs regulates mural cell recruitment to the developing CNS vasculature, which is crucial for formation and stability of blood vessels during development [1,22,23], and plays a role in maintaining BBB integrity in the adult brain [24,25]. Both pericytes and SMCs express PDGFR $\beta$  during development [22,23], whereas in the adult brain PDGFR $\beta$  is expressed at higher levels in pericytes compared to SMCs as shown in human tissue [26], human pericyte and SMCs cultures [27], and murine models [28,29].

Pericytes are centrally positioned within the NVU, and are highly vulnerable to different types of cellular stress [1]. Chronic loss of pericytes disrupts BBB and cerebral blood flow regulation [1,6,7,24,25,30]. Moreover, acute pericyte ablation in mice leads to circulatory failure with loss of blood flow and loss of neurotrophic support, which together leads to rapid neuron loss, neurodegenerative changes and behavioral deficits [29]. Pericyte injury results in cleavage of soluble PDGFR $\beta$  (sPDGFR $\beta$ ) [27] that is detectable in human and murine cerebrospinal fluid (CSF) [31,32]. Moreover, CSF sPDGFR $\beta$  levels are increased in

humans during the early stages of cognitive impairment, which correlates with BBB breakdown, as shown by dynamic contrast-enhanced magnetic resonance imaging in the hippocampus of the living human brain in individuals with mild cognitive impairment [31,32]. These studies support that BBB breakdown and pericyte injury measured by CSF sPDGFR $\beta$  are early biomarkers of human cognitive dysfunction [31,32]. However, whether lower levels of sPDGFR $\beta$  in CSF can predict and/or associate with slower cognitive decline, is currently unknown and remains to be explored by future studies.

Here, we developed a highly sensitive immunoassay to quantify sPDGFR $\beta$  levels in human CSF using the Meso Scale Discovery (MSD) electrochemiluminescence platform. A combination of reagents and conditions were tested, optimized, and validated. This included five capture and three detection PDGFR $\beta$  antibodies and two recombinant protein standards. The study identified the combination of reagents and conditions that yielded optimal results for an immunoassay with the large dynamic range of detection from 100–26,000 pg/mL, and intra- and inter-assay coefficient of variation <5%. Using this new assay, we present preliminary findings showing elevated CSF sPDGFR $\beta$  levels in individuals with early cognitive impairment, supporting our earlier findings that sPDGFR $\beta$  is a promising and sensitive early biomarker of human cognitive dysfunction [31,32]. These findings should be further validated by a larger prospective study. The assay could be applied at different laboratories to facilitate diagnostic and therapeutic studies of brain pericyte and BBB disruption in relation to cognition in brain disorders associated with neurovascular dysfunction and cognitive impairment.

## 2. METHODS

### 2.1. The sPDGFR $\beta$ Assay

We used the following reagents: Standard bind 96-well plates (Catalog no. L15XA-3, MSD, Rockville, Maryland); High bind 96-well plates (Catalog no. L15XB-1/L11XB-1, MSD); the following *capture antibodies*: human PDGFR $\beta$  polyclonal goat immunoglobulin G (IgG) against amino acids 33–530 (Catalog no. AF385, R&D Systems, Minneapolis, MN); human PDGFR $\beta$  monoclonal mouse IgG raised against recombinant human PDGFR $\beta$  protein (Catalog no. MA5–15103, Thermo Fisher Scientific, Rockford, IL); human PDGFR $\beta$  polyclonal rabbit IgG against amino acids 54–72 (Catalog no. PA1–30317, Thermo Fisher Scientific); human PDGFR $\beta$  monoclonal mouse IgG against PDGFR $\beta$  protein in human skin fibroblast extracts (Catalog no. MAB1263, R&D Systems); human PDGFR $\beta$  monoclonal mouse IgG raised against amino acids 33–531 (Catalog no. MAB385, R&D Systems); the following *detection antibodies*: human PDGFR $\beta$  biotinylated polyclonal IgG against amino acids 33–530 (Catalog no. BAF385, R&D Systems); mouse PDGFR $\beta$  biotinylated polyclonal IgG against amino acids 32–530 and having approximately 40% cross-reactivity with recombinant human PDGFR $\beta$  (Catalog no. BAF1042, R&D Systems); human PDGFR $\beta$  polyclonal rabbit IgG raised against amino acids 54–72 (Catalog no. PA1–30317, Thermo Fisher Scientific); the following *standard proteins*: recombinant PDGFR $\beta$  human protein without catalytic activity domain (Catalog no. 10514H08H50, Invitrogen, Carlsbad, CA); carrier free recombinant human PDGFR $\beta$  Fc chimera (Catalog no. 385-PR/CF, R&D Systems); Blocker B (Catalog no. R93BB-2, MSD); Sulfo-tag labeled streptavidin (Catalog

no. R32AD, MSD); Sulfo-tag labeled goat anti-rabbit IgG (Catalog no. R32AB, MSD); Read Buffer T with surfactant (Catalog no. R92TC-3, MSD); adhesive seal (Microseal<sup>®</sup>, Catalog no. MSB1001, Bio-Rad, Hercules, CA).

We developed a new sandwich immunoassay to quantify sPDGFR $\beta$  levels in human CSF using the MSD platform. First, standard-bind 96-well plates were coated with a capture antibody against the extracellular domain of human PDGFR $\beta$ . Each well was spot-coated with 5  $\mu$ L of 40  $\mu$ g/mL of human PDGFR $\beta$  polyclonal goat IgG prepared in 0.01 M phosphate-buffered saline (PBS) pH 7.4 + 0.03% Triton X-100. The plate was placed uncovered on a flat surface to allow the spot coating solution to air-dry overnight at room temperature. The plates were blocked with 150  $\mu$ L per well of 1% Blocker B or an equivalent milk-based solution prepared in 0.01 M PBS pH 7.4 + 0.05% Tween-20. The plate was sealed with an adhesive seal and incubated at room temperature for 1 hour on an orbital plate shaker (~500 rpm). The plate was washed three times with 200  $\mu$ L/well of wash buffer (0.01 M PBS pH 7.4 + 0.05% Tween-20) and tapped on an absorbent pad to remove residual wash buffer. Blocker B diluent (0.2%) was prepared in wash buffer immediately before use and used to dilute standards and samples. For the standard, we used PDGFR $\beta$  recombinant human protein without catalytic activity domain at a stock concentration of 0.5  $\mu$ g/ $\mu$ L. The following standard concentrations were prepared and used in the assay: 6400, 3200, 1600, 800, 400, 200, 100 pg/mL. The diluent was used as the zero standard. Standards were mixed well by vortexing between each serial dilution step. For human CSF samples, we prepared 1:2 dilutions in 0.2% Blocker B diluent in polypropylene protein low-bind tubes. Twenty-five  $\mu$ L of prepared standards or samples were pipetted into pre-designated wells in duplicate. The plate was sealed and incubated at 4°C overnight on an orbital plate shaker (~500 rpm). The plate was washed three times with 200  $\mu$ L/well of wash buffer and tapped on an absorbent pad to remove residual wash buffer. The detection antibody solution was prepared by combining 1  $\mu$ g/mL of human PDGFR $\beta$  biotinylated antibody, and 1  $\mu$ g/mL of Sulfo-tag labeled streptavidin in 0.2% Blocker B diluent; prepared on ice immediately before use. Twenty-five  $\mu$ L of the detection antibody solution was pipetted into each well, and the sealed plate was incubated at room temperature for 1.5 hours on an orbital plate shaker (~500 rpm). The plate was washed three times with 200  $\mu$ L/well of wash buffer and tapped on an absorbent pad to remove residual wash buffer. Read Buffer T (2x) with surfactant was prepared in ddH<sub>2</sub>O, and 150  $\mu$ L was pipetted into each well carefully avoiding the introduction of air bubbles. The plate was read immediately on the MSD SECTOR Imager 6000 with electrochemiluminescence detection. The raw readings were analyzed by subtracting the average background value of the zero standard from each recombinant standard and sample readings. A standard curve was constructed by plotting the recombinant standard readings and their known concentrations and applying a linear curve fit. The sPDGFR $\beta$  concentrations were calculated using the samples' reading and the linear standard curve equation; the result was corrected for the sample dilution factor to arrive at the sPDGFR $\beta$  concentration in the original CSF samples.

## 2.2. Validation Parameters

To validate the immunoassay's performance, we tested detection limits, dilutional linearity, parallelism, spiked recovery, precision (including repeatability and reproducibility), and

robustness, as reported in the guide to immunoassay method validation [33]. Each of these features are described below.

Detection limits are the lower and upper limits of detection and the lowest and highest amount of analyte in a sample that can be detected, respectively, and were determined from the CSF samples analyzed.

Dilutional linearity is the ability to obtain analyte concentration test results that are directly proportional to the performed sample dilution. This was tested to validate that sample dilution does not affect accuracy and precision. Tests of dilutional linearity results in a low coefficient of variation (CV) of analyte concentration measured from the same homogeneous sample at different dilutions.

Parallelism was tested to determine that the sample dilution response curve is parallel to the standard concentration response curve over a range of dilutions, which is an important validation parameter to ensure that test samples do not result in biased measurements of the analyte concentration.

Spiked recovery is the close agreement between the accepted conventional true analyte value (biological sample spiked with known analyte concentration) and the value found in the test sample (recovery of biological and spiked analyte).

Precision refers to the close agreement between independent test results from replicate determinations of the same homogeneous sample under the normal assay conditions, and is comprised of intermediate precision, repeatability and reproducibility. Since precision is difficult to quantify, we therefore measured and reported imprecision by the intra-assay and inter-assay CV. Measures of intra-assay CV was performed for 21 CSF samples and the average value is reported. Measures of inter-assay CV was performed for 80 CSF samples and the average value is reported.

Robustness is the measure of a method's capacity to remain unaffected by small variations in method parameters [33], and it was tested by shortening detection antibody incubation from 1.5 hours to 1 hour and also by storing plates pre-coated with capture antibody for up to one month at 4°C prior to conducting the assay.

### 2.3 Human Study Participants

Participants were recruited through the University of Southern California (USC) Alzheimer's Disease Research Center (ADRC) in Los Angeles, CA, and the Washington University Knight ADRC in St. Louis, MO. Inclusion criteria were males and females from ages 46 to 92, with Clinical Dementia Rating (CDR) global scores of 0, 0.5, or 1, corresponding to unimpaired cognition, mild cognitive impairment, and mild dementia, respectively, who were enrolled through the USC Alzheimer's Disease Research Center (ADRC) in Los Angeles, CA, and the Washington University Knight ADRC in St. Louis, MO (funded by the NIA program P01AG052350), who had lumbar punctures and venipunctures, and were evaluated using the Uniform Data Set (UDS) [34] and supplemental neuropsychological tests. Neuropsychological testing was conducted in accordance with standardized procedures [35]. A total of 147 individuals are included in this study. The

participants' Clinical Dementia Rating (CDR) [36] score was obtained through standardized interview and assessment with the participant and a knowledgeable informant following UDS procedures.

Individuals were excluded if they had moderate-to-severe dementia ( $CDR > 1$ ) or primary etiologic diagnoses not related to AD, including vascular cognitive impairment, vascular dementia, Lewy body dementia, frontotemporal lobar degeneration, traumatic brain injury, Huntington disease, Down syndrome, Parkinson's disease, normal pressure hydrocephalus, neoplasm, human immunodeficiency virus (HIV), substance abuse, hypothyroidism, or medication use likely to affect brain function.

All participants and/or legally authorized representatives, and study partners provided informed consent or proxy informed consent if warranted. The study was approved by the Institutional Review Boards of USC and Washington University.

#### 2.4. Collection of Biofluids

Participants underwent lumbar puncture and venipuncture in the morning following an overnight fast. The CSF was collected by gravity drip in polypropylene tubes, processed (centrifuged at 2000 g, 10 minutes, 4°C), aliquoted at 500  $\mu$ L into polypropylene tubes, and immediately stored at  $-80^{\circ}\text{C}$  until assay. Blood was collected into ethylenediaminetetraacetic acid (EDTA) tubes and processed (centrifuged at 2000 g, 10 minutes, 4°C). Plasma and the buffy coat were aliquoted in polypropylene tubes and stored at  $-80^{\circ}\text{C}$ ; buffy coat was used for DNA extraction and *APOE* genotyping.

#### 2.5. *APOE* Genotyping

DNA was extracted from buffy coat using the Quick-gDNA Blood Miniprep Kit (Catalog no. D3024, Zymo Research, Irvine, CA). *APOE* genotyping was performed via polymerase chain reaction (PCR)-based retention fragment length polymorphism analysis, as previously reported [32].

#### 2.6. Molecular Biofluid Assays

Albumin quotient (Qalb, the ratio of CSF-to-plasma albumin levels) was determined using enzyme-linked immunosorbent assay (ELISA) (Catalog no. E-80AL, Immunology Consultants Laboratory, Inc., Portland, OR). CSF levels of fibrinogen were determined by ELISA (Catalog no. E-80FIB, Immunology Consultants Laboratory, Inc.). CSF levels of plasminogen were determined by ELISA (Catalog no. E-80PMG, Immunology Consultants Laboratory, Inc.).

#### 2.6. Statistical Analysis

For comparison between two groups, statistical significance was analyzed by unpaired two-tailed Student's t-test. For multiple comparisons, one-way analysis of variance (ANOVA) followed by Tukey's posthoc test was used. Data was normally distributed with homogeneous variances, supporting the use of parametric statistics. Linear regression analysis was used to assess the significance of correlations, and the Pearson correlation



coefficient was determined.  $P < 0.05$  was considered significant. Statistical analyses were conducted using GraphPad Prism 7.0 software. Single data points are plotted in the figures.

### 3. RESULTS

We developed a new assay to detect the soluble extracellular domain of PDGFR $\beta$  using electrochemiluminescence detection on the MSD platform. A combination of reagents and conditions were tested, optimized, and validated. Table 1 summarizes the reagents tested (i.e., plate types, block solutions, recombinant standards, capture antibodies, and detection antibodies) and identifies the combination of conditions that yielded optimal results (denoted with asterisks). The optimal reagent combination was then validated to generate a standard operating procedure.

To validate the assay, we tested detection limits, dilutional linearity, parallelism, spiked recovery, precision (including repeatability, intermediate precision, and reproducibility), and robustness (Table 2) [33]. Two different recombinant PDGFR $\beta$  standard proteins exhibited a large, dynamic linear curve fit ranging from 100 – 26,000 pg/mL with a coefficient of linearity ( $r^2$ ) of 0.9996 and 0.996 (Fig. 1a), and all CSF samples measured fell within the assay's standard curve range of detection. Additionally, there was excellent dilutional linearity of CSF samples diluted from 1:2–1:16 (average CV 2.55%) (Fig. 1b), indicating that the dilutions yielded consistent results within the desirable assay range. Next, parallelism measures revealed parallel response curves of samples and the standard across the dilution range (Fig. 1c), demonstrating that the test sample dilution does not result in a biased measurement of the analyte concentration. Imprecision was quantified by intra-assay and inter-assay CV of the same sample assayed under the standard operating procedure (see Methods section 2.1 The sPDGFR $\beta$  Assay for procedural details), resulting in an average CV of 4.71% and 4.60%, respectively. Reproducibility of the assay was tested by conducting the standard operating procedures over a range of three years and by different laboratory personnel, which, in all instances, yielded CV less than 10% which is within acceptable criteria for immunoassay CV thresholds [33,37,38]. Finally, to validate the assay's robustness, we varied the standard operating procedures by shortening the detection antibody incubation from 1.5 hours to 1 hour and also by storing plates pre-coated with capture antibody for up to one month at 4°C prior to conducting the assay. In both instances, the assay performance was unaffected and resulted in the same analyte concentration measured (within the <10% CV threshold) independent of the procedural variations, which indicates robustness of the assay. In summary, the new sPDGFR $\beta$  assay yields exceptional sensitivity with a lower detection limit of 100 pg/mL, and the assay produces remarkable precision with low intra- and inter-assay CVs (Fig. 1d).

A total of 147 individuals with normal cognition (CDR 0), mild cognitive impairment (CDR 0.5), and mild dementia (CDR 1) were included in the study. Table 3 presents demographic and clinical data of participants grouped by global CDR score, with the following parameters reported: global CDR score, number of participants, mean age at lumbar puncture, percent female, and percent *APOE4* carriers. Using this assay, we found that CSF sPDGFR $\beta$  levels are significantly elevated in individuals with mild cognitive impairment (CDR 0.5) and mild dementia (CDR 1) compared to cognitively normal (CDR 0) individuals



(Fig. 2a), indicating brain microvascular pericyte injury during early stages of cognitive impairment as previously reported [31,32]. Pericyte injury and BBB breakdown are related events [31,32], as confirmed here by positive correlations of CSF sPDGFR $\beta$  with traditional biomarkers of BBB breakdown, including Qalb, CSF fibrinogen and CSF plasminogen levels (Fig. 2b–d). Finally, since our earlier work used quantitative Western blot analysis to determine sPDGFR $\beta$  levels in the CSF (see representative standard curve, Fig. 2e) [31,32], we next measured sPDGFR $\beta$  levels in the same CSF samples by quantitative Western blotting and our new immunoassay, which revealed a positive correlation (Fig. 2f), as an additional validation step of the new assay's performance and relevance to existing literature.

#### 4. DISCUSSION

We developed new highly sensitive and reproducible immunoassay to quantify sPDGFR $\beta$  levels in human CSF. The present results support previous findings showing elevated CSF sPDGFR $\beta$  levels in individuals that are at increased risk of developing early cognitive impairment [31,32]. Since our study is based on relatively limited number of subjects (i.e., 147) from two centers, we consider these results as valuable preliminary findings that should be further validated by larger prospective studies in AD-like populations, as well as for indications beyond AD, including other neurodegenerative disorders associated with microvascular and cognitive dysfunction.

Although the present findings would be strengthened by the addition of more pericyte markers, the additional pericyte-specific markers presently do not exist. There is a paucity of unique identifiable markers that are pericyte-specific, since pericytes share many markers with other cell types including SMC [1,3,28,29]. Yet, upon insult, pericytes are the predominant source of shedded soluble sPDGFR $\beta$  that can be measured in CSF as we reported both in humans and animal models [27,31,32], indicating that CSF sPDGFR $\beta$  is specific to pericyte injury.

We and others have also shown that pericyte injury, measured singly by CSF sPDGFR $\beta$ , is associated with BBB breakdown as measured by neuroimaging biomarkers and classical molecular CSF biomarkers of BBB breakdown (e.g., albumin quotient, fibrinogen), which increases with cognitive impairment and Alzheimer's disease [31,32,39]. These studies also revealed that CSF sPDGFR $\beta$  is an early biomarker of human cognitive dysfunction independent of Alzheimer's A $\beta$  and tau pathways [31,32], which demands development of an improved, reproducible sPDGFR $\beta$  immunoassay.

Compared with existing approaches to detect sPDGFR $\beta$  by either quantitative Western blot [31,32] or the only commercially available assay (Thermo Fisher Scientific), our new MSD-based assay has favorable features such as *i*) high throughput, *ii*) requires significantly less CSF sample volume, *iii*) has a large dynamic range of detection, *iv*) is time and cost effective, *v*) has high precision and accuracy, and *vi*) has the capability to be multiplexed with other key analytes for research or clinical utility (Table 4). Additionally, our novel MSD-based sPDGFR $\beta$  assay is easy to incorporate at different laboratories to investigate pericyte and BBB injury in various cohorts.

The biomarker field is beginning to see a push for blood-based biomarkers and automation. The large dynamic range of the present sPDGFR $\beta$  assay suggests that it will likely be able to detect changes in plasma sPDGFR $\beta$ , but this remains to be confirmed by future studies. A recent study using ELISA found that serum and CSF levels of sPDGFR $\beta$  are positively correlated, and that CSF sPDGFR $\beta$  levels are increased in AD, which correlated with BBB breakdown as determined with Qalb [39]. Further testing and validation, however, is needed to determine clinical relevance of sPDGFR $\beta$  in blood in relation to cognition and BBB breakdown in individuals with cognitive dysfunction, AD and other neurological disorders. Additionally, automated immunoassays are ideal for ease of clinical use and enhanced speed and accuracy, but initially automated immunoassays are only being developed for standard AD biomarkers and they are not yet widely accepted and incorporated into either research use or clinical practice. If or when automation become the ‘gold standard’ in the future, an sPDGFR $\beta$  assay could then be developed to further enable clinical measures of microvascular dysfunction.

Our new assay detects the soluble extracellular portion of PDGFR $\beta$ . Ligands predominantly bind to Ig-like domains 2 and 3 causing receptor dimerization, and the receptor dimer is further stabilized by direct receptor-receptor interactions of Ig-like domain 4 [40–42]. To date the 3-dimensional structure of PDGFR $\beta$  has not been resolved, nor has the precise mechanism(s) of the PDGFR $\beta$  ectodomain shedding from pericytes been elucidated. Recent evidence indicates that a disintegrin and metalloproteinase (ADAM) family member, ADAM10, can mediate sPDGFR $\beta$  shedding from pericytes but not SMCs [32], consistent with another study showing ADAM10 sheds sPDGFR $\beta$  in fibroblasts [43]. While ADAM10 plays a role in PDGFR $\beta$  shedding from pericytes [32], it is currently elusive whether ADAM17 or other enzymes are also involved. Further, it is presently unknown whether the extracellular domain of PDGFR $\beta$  is internalized or cleaved into the soluble form prior to receptor internalization. Elucidating the exact mechanism(s) underlying ectodomain shedding of PDGFR $\beta$  in response to pericyte injury would not only inform the degree to which sPDGFR $\beta$  is detectable as a result of pericyte dysfunction versus degeneration but also has the potential to identify novel therapeutic targets. However, these studies are outside the scope of the present report.

Given the lack of additional pericyte-specific markers and in light of the growing evidence that cerebrovascular and BBB dysfunction contributes to cognitive impairment and dementia, including AD [2,3,5–10,31,32], this new assay for detection of a biomarker of pericyte injury in biofluids will be impactful for the field’s efforts to combat numerous brain disorders with vascular contributions to cognitive impairment and dementia. The assay could be applied at different laboratories to study brain pericyte injury and microvascular damage in relation to cognitive decline in disorders associated with neurovascular and cognitive dysfunction.

## CONCLUSION

This study describes a new immunoassay offering a highly reproducible and quantitative analysis of sPDGFR $\beta$  levels in human CSF. The overall results support our previous findings [31,32] showing that CSF sPDGFR $\beta$  is a promising early biomarker of human cognitive

dysfunction. Since, sPDGFR $\beta$  is a biomarker of brain pericyte and BBB injury, this new assay will allow future diagnostic and/or therapeutic studies of brain microvascular damage in relation to cognition in different neurodegenerative disorders associated with neurovascular dysfunction. We envision this assay would first be used clinically to target AD-like populations as a measure of microvascular and pericyte injury related to cognitive decline. Subsequently, in addition to AD, it will also be relevant to employ this sPDGFR $\beta$  assay in Parkinson's disease, Huntington disease, HIV-dementia, or post-traumatic brain injury related dementia [3,6], as well as various types of vascular dementia including small vessel disease of the brain and other vascular contributions to cognitive impairment and dementia (VCID) [4,9]. We hope that the present preliminary findings will encourage further these prospective and therapeutic studies in different clinical cohorts.

## ACKNOWLEDGEMENTS

M.D.S., A.P.S., and B.V.Z. designed the study approach and interpreted the data. M.D.S. and A.P.S. performed experiments and analyzed the data. M.P., M.G.H., E.J., H.C.C., L.S.S., J.M.R., A.M.F., J.C.M., and A.W.T. recruited the participants. M.G.H., L.S.S., A.M., A.M.F., J.C.M., J.P., D.A.N., and A.W.T provided critical reading of the manuscript. M.D.S. and B.V.Z. wrote the manuscript.

Development of new sPDGFR $\beta$  assay was supported by the National Institutes of Health (NIH) grant 5P01AG052350 to B.V.Z. and A.W.T. and the Zilkha Neurogenetic Institute Research Funds. Cerebrospinal fluid samples, clinical evaluation and cognitive assessment data were obtained from participants recruited through the University of Southern California Alzheimer's Disease Research Center (ADRC) in Los Angeles, CA, and the Washington University Knight ADRC in St. Louis, MO, supported by the grants 5P01AG052350 to B.V.Z. and A.W.T., 5P50AG005142 to H.C.C., and P50AG05681, P01AG03991, and P01AG026272 to J.C.M. M.G.H. is supported by the L.K. Whittier Foundation.

## REFERENCES

- [1]. Sweeney MD, Ayyadurai S, Zlokovic BV. Pericytes of the neurovascular unit: key functions and signaling pathways. *Nat Neurosci* 2016;19:771–83. doi:10.1038/nn.4288. [PubMed: 27227366]
- [2]. Zlokovic BV. Neurovascular pathways to neurodegeneration in Alzheimer's disease and other disorders. *Nat Rev Neurosci* 2011;12:723–38. doi:10.1038/nrn3114. [PubMed: 22048062]
- [3]. Sweeney MD, Zhao Z, Montagne A, Nelson AR, Zlokovic BV. Blood-Brain Barrier: From Physiology to Disease and Back. *Physiol Rev* 2019;99:21–78. doi:10.1152/physrev.00050.2017. [PubMed: 30280653]
- [4]. Iadecola C The Neurovascular Unit Coming of Age: A Journey through Neurovascular Coupling in Health and Disease. *Neuron* 2017;96:17–42. doi:10.1016/j.neuron.2017.07.030. [PubMed: 28957666]
- [5]. Sweeney MD, Sagare AP, Zlokovic BV. Blood-brain barrier breakdown in Alzheimer disease and other neurodegenerative disorders. *Nat Rev Neurol* 2018;14:133–50. doi:10.1038/nrneurol.2017.188. [PubMed: 29377008]
- [6]. Sweeney MD, Kisler K, Montagne A, Toga AW, Zlokovic BV. The role of brain vasculature in neurodegenerative disorders. *Nat Neurosci* 2018;21:1318–31. doi:10.1038/s41593-018-0234-x. [PubMed: 30250261]
- [7]. Kisler K, Nelson AR, Montagne A, Zlokovic BV. Cerebral blood flow regulation and neurovascular dysfunction in Alzheimer disease. *Nat Rev Neurosci* 2017;18:419–34. doi:10.1038/nrn.2017.48. [PubMed: 28515434]
- [8]. Montagne A, Nation DA, Pa J, Sweeney MD, Toga AW, Zlokovic BV. Brain imaging of neurovascular dysfunction in Alzheimer's disease. *Acta Neuropathol* 2016;131:687–707. doi:10.1007/s00401-016-1570-0. [PubMed: 27038189]
- [9]. Sweeney MD, Montagne A, Sagare AP, Nation DA, Schneider LS, Chui HC, et al. Vascular dysfunction-The disregarded partner of Alzheimer's disease. *Alzheimers Dement* 2019;15:158–67. doi:10.1016/j.jalz.2018.07.222. [PubMed: 30642436]

- [10]. Iturria-Medina Y, Sotero RC, Toussaint PJ, Mateos-Pérez JM, Evans AC, Alzheimer's Disease Neuroimaging Initiative. Early role of vascular dysregulation on late-onset Alzheimer's disease based on multifactorial data-driven analysis. *Nat Commun* 2016;7:11934. doi:10.1038/ncomms11934. [PubMed: 27327500]
- [11]. Salloway S, Gur T, Berzin T, Tavares R, Zipser B, Correia S, et al. Effect of APOE genotype on microvascular basement membrane in Alzheimer's disease. *J Neurol Sci* 2002;203–204:183–7.
- [12]. Zipser BD, Johanson CE, Gonzalez L, Berzin TM, Tavares R, Hulette CM, et al. Microvascular injury and blood-brain barrier leakage in Alzheimer's disease. *Neurobiol Aging* 2007;28:977–86. doi:10.1016/j.neurobiolaging.2006.05.016. [PubMed: 16782234]
- [13]. Ryu JK, McLarnon JG. A leaky blood-brain barrier, fibrinogen infiltration and microglial reactivity in inflamed Alzheimer's disease brain. *J Cell Mol Med* 2009;13:2911–25. doi:10.1111/j.1582-4934.2008.00434.x. [PubMed: 18657226]
- [14]. Farrall AJ, Wardlaw JM. Blood-brain barrier: ageing and microvascular disease--systematic review and meta-analysis. *Neurobiol Aging* 2009;30:337–52. doi:10.1016/j.neurobiolaging.2007.07.015. [PubMed: 17869382]
- [15]. Hultman K, Strickland S, Norris EH. The APOE  $\epsilon 4/\epsilon 4$  genotype potentiates vascular fibrin(ogen) deposition in amyloid-laden vessels in the brains of Alzheimer's disease patients. *J Cereb Blood Flow Metab* 2013;33:1251–8. doi:10.1038/jcbfm.2013.76. [PubMed: 23652625]
- [16]. Sengillo JD, Winkler EA, Walker CT, Sullivan JS, Johnson M, Zlokovic BV. Deficiency in mural vascular cells coincides with blood-brain barrier disruption in Alzheimer's disease. *Brain Pathol* 2013;23:303–10. doi:10.1111/bpa.12004. [PubMed: 23126372]
- [17]. Halliday MR, Rege SV, Ma Q, Zhao Z, Miller CA, Winkler EA, et al. Accelerated pericyte degeneration and blood-brain barrier breakdown in apolipoprotein E4 carriers with Alzheimer's disease. *J Cereb Blood Flow Metab* 2016;36:216–27. doi:10.1038/jcbfm.2015.44. [PubMed: 25757756]
- [18]. Farkas E, Luiten PG. Cerebral microvascular pathology in aging and Alzheimer's disease. *Prog Neurobiol* 2001;64:575–611. [PubMed: 11311463]
- [19]. Baloyannis SJ, Baloyannis IS. The vascular factor in Alzheimer's disease: a study in Golgi technique and electron microscopy. *J Neurol Sci* 2012;322:117–21. doi:10.1016/j.jns.2012.07.010. [PubMed: 22857991]
- [20]. Halliday MR, Pomara N, Sagare AP, Mack WJ, Frangione B, Zlokovic BV. Relationship between cyclophilin A levels and matrix metalloproteinase 9 activity in cerebrospinal fluid of cognitively normal apolipoprotein e4 carriers and blood-brain barrier breakdown. *JAMA Neurol* 2013;70:1198–200. doi:10.1001/jamaneurol.2013.3841. [PubMed: 24030206]
- [21]. Zonneveld HI, Goos JDC, Wattjes MP, Prins ND, Scheltens P, van der Flier WM, et al. Prevalence of cortical superficial siderosis in a memory clinic population. *Neurology* 2014;82:698–704. doi:10.1212/WNL.000000000000150. [PubMed: 24477113]
- [22]. Armulik A, Genové G, Betsholtz C. Pericytes: developmental, physiological, and pathological perspectives, problems, and promises. *Dev Cell* 2011;21:193–215. doi:10.1016/j.devcel.2011.07.001. [PubMed: 21839917]
- [23]. Hellström M, Kalén M, Lindahl P, Abramsson A, Betsholtz C. Role of PDGF-B and PDGFR-beta in recruitment of vascular smooth muscle cells and pericytes during embryonic blood vessel formation in the mouse. *Development* 1999;126:3047–55. [PubMed: 10375497]
- [24]. Armulik A, Genové G, Mäe M, Nisancioglu MH, Wallgard E, Niaudet C, et al. Pericytes regulate the blood-brain barrier. *Nature* 2010;468:557–61. doi:10.1038/nature09522. [PubMed: 20944627]
- [25]. Bell RD, Winkler EA, Sagare AP, Singh I, LaRue B, Deane R, et al. Pericytes control key neurovascular functions and neuronal phenotype in the adult brain and during brain aging. *Neuron* 2010;68:409–27. doi:10.1016/j.neuron.2010.09.043. [PubMed: 21040844]
- [26]. Miners JS, Schulz I, Love S. Differing associations between A $\beta$  accumulation, hypoperfusion, blood-brain barrier dysfunction and loss of PDGFRB pericyte marker in the precuneus and parietal white matter in Alzheimer's disease. *J Cereb Blood Flow Metab* 2018;38:103–15. doi:10.1177/0271678X17690761. [PubMed: 28151041]

- [27]. Sagare AP, Sweeney MD, Makshanoff J, Zlokovic BV. Shedding of soluble platelet-derived growth factor receptor- $\beta$  from human brain pericytes. *Neurosci Lett* 2015;607:97–101. doi:10.1016/j.neulet.2015.09.025. [PubMed: 26407747]
- [28]. Vanlandewijck M, He L, Mäe MA, Andrae J, Ando K, Del Gaudio F, et al. A molecular atlas of cell types and zonation in the brain vasculature. *Nature* 2018;554:475–80. doi:10.1038/nature25739. [PubMed: 29443965]
- [29]. Nikolakopoulou AM, Montagne A, Kisler K, Dai Z, Wang Y, Huuskonen MT, et al. Pericyte loss leads to circulatory failure and pleiotrophin depletion causing neuron loss. *Nat Neurosci* 2019;22:1089–98. doi:10.1038/s41593-019-0434-z. [PubMed: 31235908]
- [30]. Kisler K, Nelson AR, Rege SV, Ramanathan A, Wang Y, Ahuja A, et al. Pericyte degeneration leads to neurovascular uncoupling and limits oxygen supply to brain. *Nat Neurosci* 2017;20:406–16. doi:10.1038/nn.4489. [PubMed: 28135240]
- [31]. Montagne A, Barnes SR, Sweeney MD, Halliday MR, Sagare AP, Zhao Z, et al. Blood-brain barrier breakdown in the aging human hippocampus. *Neuron* 2015;85:296–302. doi:10.1016/j.neuron.2014.12.032. [PubMed: 25611508]
- [32]. Nation DA, Sweeney MD, Montagne A, Sagare AP, D’Orazio LM, Pachicano M, et al. Blood-brain barrier breakdown is an early biomarker of human cognitive dysfunction. *Nat Med* 2019;25:270–6. doi:10.1038/s41591-018-0297-y. [PubMed: 30643288]
- [33]. Andreasson U, Perret-Liaudet A, van Waalwijk van Doorn LJC, Blennow K, Chiasserini D, Engelborghs S, et al. A Practical Guide to Immunoassay Method Validation. *Front Neurol* 2015;6:179. doi:10.3389/fneur.2015.00179. [PubMed: 26347708]
- [34]. Weintraub S, Salmon D, Mercaldo N, Ferris S, Graff-Radford NR, Chui H, et al. The Alzheimer’s Disease Centers’ Uniform Data Set (UDS): the neuropsychologic test battery. *Alzheimer Dis Assoc Disord* 2009;23:91–101. doi:10.1097/WAD.0b013e318191c7dd. [PubMed: 19474567]
- [35]. Alzheimer’s Disease Neuroimaging Initiative. Procedures Manual [Internet]. [cited 2015 Mar 11]. Available from: <https://adni.loni.usc.edu/wp-content/uploads/2008/07/adni2-procedures-manual.pdf>
- [36]. Morris JC. The Clinical Dementia Rating (CDR): current version and scoring rules. *Neurology* 1993;43:2412–4.
- [37]. Janelidze S, Stomrud E, Palmqvist S, Zetterberg H, van Westen D, Jeromin A, et al. Plasma  $\beta$ -amyloid in Alzheimer’s disease and vascular disease. *Sci Rep* 2016;6:26801. doi:10.1038/srep26801. [PubMed: 27241045]
- [38]. Semenova VA, Schiffer J, Steward-Clark E, Soroka S, Schmidt DS, Brawner MM, et al. Validation and long term performance characteristics of a quantitative enzyme linked immunosorbent assay (ELISA) for human anti-PA IgG. *J Immunol Methods* 2012;376:97–107. doi:10.1016/j.jim.2011.12.002. [PubMed: 22197974]
- [39]. Miners JS, Kehoe PG, Love S, Zetterberg H, Blennow K. CSF evidence of pericyte damage in Alzheimer’s disease is associated with markers of blood-brain barrier dysfunction and disease pathology. *Alzheimers Res Ther*; In Press.
- [40]. Heldin C-H. Targeting the PDGF signaling pathway in tumor treatment. *Cell Commun Signal* 2013;11:97. doi:10.1186/1478-811X-11-97. [PubMed: 24359404]
- [41]. Yang Y, Yuzawa S, Schlessinger J. Contacts between membrane proximal regions of the PDGF receptor ectodomain are required for receptor activation but not for receptor dimerization. *Proc Natl Acad Sci USA* 2008;105:7681–6. doi:10.1073/pnas.0802896105. [PubMed: 18505839]
- [42]. Omura T, Heldin CH, Ostman A. Immunoglobulin-like domain 4-mediated receptor-receptor interactions contribute to platelet-derived growth factor-induced receptor dimerization. *J Biol Chem* 1997;272:12676–82. [PubMed: 9139724]
- [43]. Mendelson K, Swendeman S, Saftig P, Blobel CP. Stimulation of platelet-derived growth factor receptor beta (PDGFRbeta) activates ADAM17 and promotes metalloproteinase-dependent cross-talk between the PDGFRbeta and epidermal growth factor receptor (EGFR) signaling pathways. *J Biol Chem* 2010;285:25024–32. doi:10.1074/jbc.M110.102566. [PubMed: 20529858]

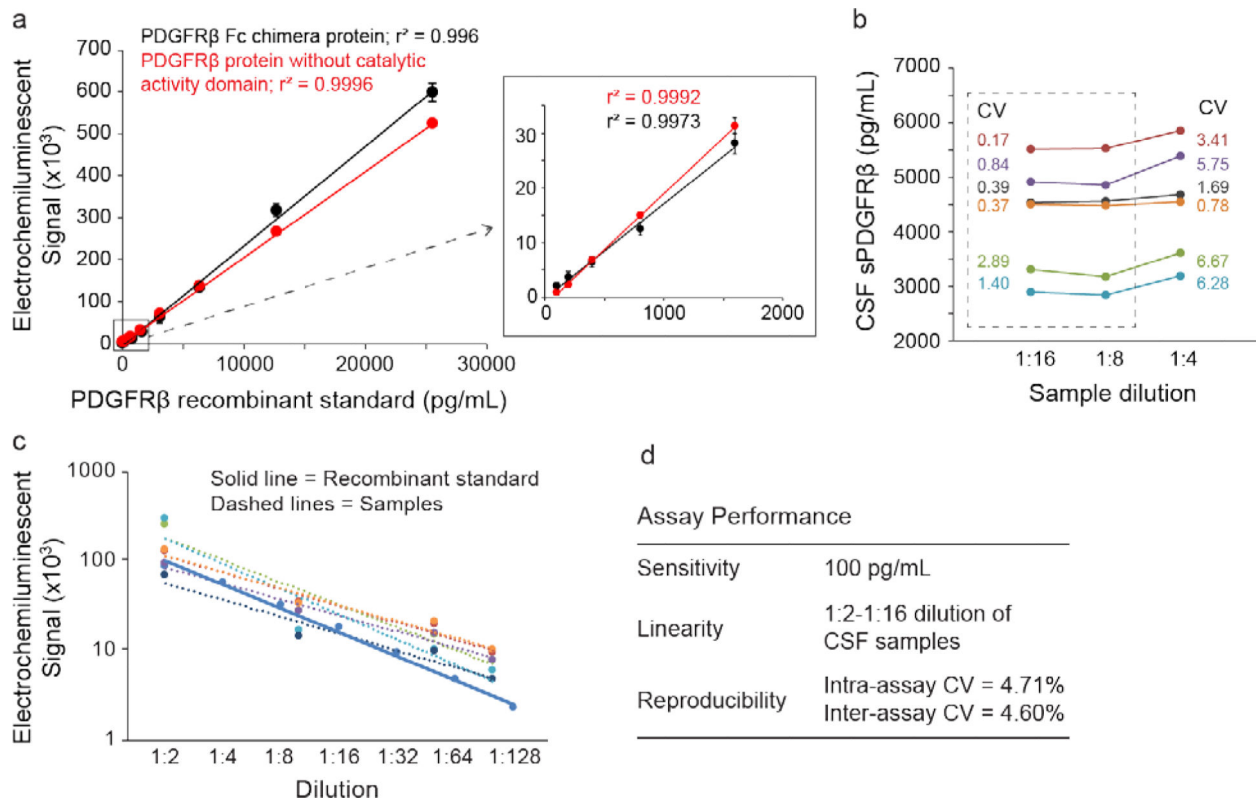


**Fig. 1. Performance summary of the novel sPDGFR $\beta$  assay.**

**a)** Representative standard curves plotting concentration and electrochemiluminescence signal of two recombinant standard proteins that both exhibit a linear curve fit over a large dynamic range from 100–26,000 pg/mL;  $r^2 = 0.996$ – $0.9996$ . The dotted gray line with arrowhead points to the graph's inset box that enlarges the lower range of the curve. Mean  $\pm$  S.D. **b)** Dilutional linearity test – CSF samples diluted 1:4, 1:8 and 1:16 have a low coefficient of variation across all sample dilutions. The left CV values are comparing samples at 1:16 and 1:8 dilutions (dotted box) and the right CV values are comparing samples at 1:8 and 1:4 dilutions. **c)** Parallelism test – the electrochemiluminescence signal of samples and the recombinant standard protein across a range of dilutions from 1:2 to 1:128 is parallel. **d)** Summary of assay performance detailing the assay's lower limit of sensitivity (100 pg/mL), sample linearity range (1:2–1:16 dilution of CSF samples), and assay reproducibility (intra- and inter-assay variability <5%) (see Methods section 2.2 Validation Parameters for additional details).



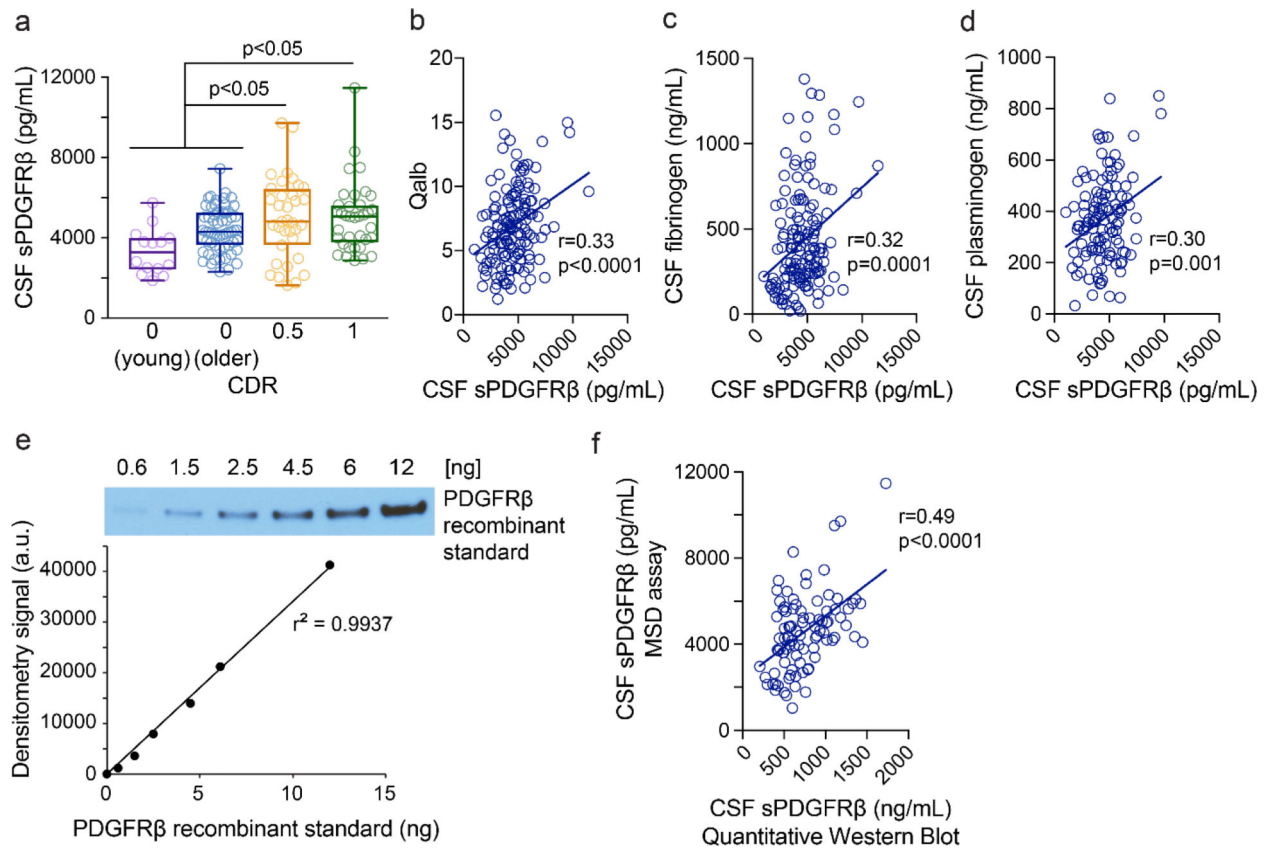


**Fig. 2. Validation of sPDGFRβ as a pericyte injury biomarker in human CSF.**

**a** CSF sPDGFRβ levels are significantly increased in individuals with CDR 0.5 (n=35) and CDR 1 (n=36) compared to cognitively normal CDR 0 individuals (n=14, young; n=59, older); significance by ANOVA with Tukey posthoc test,  $\alpha = 0.05$ . **b-d** CSF sPDGFRβ relates to blood-brain barrier breakdown as shown by positive correlations with albumin quotient (Qalb) of CSF-to-plasma albumin levels (n=143) (**b**), CSF fibrinogen (n=144) (**c**), and CSF plasminogen (n=121) (**d**). **e,f** Representative standard curve of PDGFRβ recombinant protein measured by Western blot (**e**) that is used to quantify sPDGFRβ levels in CSF samples by quantitative Western blot in panel **f**. There is a positive correlation of CSF sPDGFRβ levels measured by quantitative Western blot and the new MSD assay (n=93) (**f**). All panels plot single data points. In panel **a**, the box and whisker plots indicate the median value (horizontal line), the boxes indicate the interquartile range, and the whiskers indicate the minimum and maximum values. In panels **b-d** and **f**, Pearson correlation coefficient,  $r$ ; significance by linear regression analysis.



**Table 1.**

Summary of reagents used to develop and optimize the sPDGFR $\beta$  assay on the MSD platform. The red asterisk denotes the reagent combination that yielded optimal results.

---

Plate Type
<ul style="list-style-type: none"> <li>• Standard-bind*</li> <li>• High-bind</li> </ul>
Block Solution
<ul style="list-style-type: none"> <li>• Milk-based*</li> <li>• BSA-based</li> </ul>
Recombinant Standard
<ul style="list-style-type: none"> <li>• Recombinant hPDGFR<math>\beta</math> Fc Chimera Protein, carrier free (R&amp;D Systems #385-PR/CF)*</li> <li>• Recombinant hPDGFR<math>\beta</math> without catalytic activity domain (Invitrogen #10514H08H50)*</li> </ul>
Capture Antibody
<ul style="list-style-type: none"> <li>• hPDGFR<math>\beta</math> monoclonal mouse IgG (Thermo #MA5-15103)</li> <li>• hPDGFR<math>\beta</math> monoclonal mouse IgG (R&amp;D Systems #MAB1263)</li> <li>• hPDGFR<math>\beta</math> monoclonal mouse IgG (R&amp;D Systems #MAB385)</li> <li>• hPDGFR<math>\beta</math> polyclonal rabbit IgG (Thermo #PA1-30317)</li> <li>• hPDGFR<math>\beta</math> polyclonal goat IgG (R&amp;D Systems AF385)*</li> </ul>
Detection Antibody
<ul style="list-style-type: none"> <li>• hPDGFR<math>\beta</math> polyclonal rabbit IgG (Thermo #PA1-30317) and Sulfo-tagged goat <math>\alpha</math> rabbit IgG (MSD #R32AB)</li> <li>• Biotinylated mPDGFR<math>\beta</math> polyclonal IgG (R&amp;D Systems #BAF1042) and Sulfo-tagged streptavidin (MSD #R32AD)</li> <li>• Biotinylated hPDGFR<math>\beta</math> polyclonal goat IgG (R&amp;D Systems #BAF385) and Sulfo-tagged streptavidin (MSD #R32AD)*</li> </ul>

---

**Table 2.**

Summary of parameters used to validate performance of the new sPDGFR $\beta$  assay on the MSD platform.

Parameter	Definition	Tested
Detection limits	Lower and upper limits of detection are the lowest and highest amount of analyte in a sample that can be detected, respectively	✓
Dilution linearity	The ability to obtain analyte concentration test results that are directly proportional to the performed dilution – validates that sample dilution does not affect accuracy and precision	✓
Parallelism	Determines that the sample dilution response curve is parallel to the standard concentration response curve over a range of dilutions to ensure the test samples do not result in biased measurements of the analyte concentration	✓
Spiked recovery	Close agreement between the accepted conventional true analyte value (spiked) and the value found in the test sample (recovery)	✓
Precision	Close agreement between independent test results from replicate determinations of the same homogeneous sample under the normal assay conditions <i>a.</i> Repeatability (within-assay; within-day precision) <i>b.</i> Intermediate (between-assay; between-day repeatability) <i>c.</i> Reproducibility	✓
Robustness	A measure of the capacity of a method to remain unaffected by small variations in method parameters	✓

**Table 3.**

Participants' demographic information.

	Cognitively normal, young	Cognitively normal, older	Mild Cognitive Impairment	Mild Dementia
Clinical Dementia Rating (CDR) scale	0	0	0.5	1
Number of participants	14	59	36	38
No. USC / No. WashU	0 / 14	47 / 12	1 / 35	27 / 11
Age at LP (mean $\pm$ SD)	54.5 $\pm$ 6.2	77.45 $\pm$ 6.6	75.6 $\pm$ 5.9	76.9 $\pm$ 9.4
Female, %	50%	59%	36%	50%
<i>APOE4</i> carriers, %	50%	40%	50%	51%

Author Manuscript

Author Manuscript

Author Manuscript

Author Manuscript

**Table 4.**

Comparative performance of the new sPDGFR $\beta$  assay on the MSD platform versus other existing approaches.

	Approach to measure human sPDGFR $\beta$		
	Quantitative Western blot	Thermo Fisher Scientific ELISA	Novel assay on MSD platform
High-throughput	No	Yes	Yes
CSF volume required	Moderate (25 $\mu$ l)	High (100 $\mu$ l)	Low (7 $\mu$ l)
Large dynamic range of detection	No	No	Yes
Time & Cost	High	Low	Low
Precision & Accuracy	Moderate	High	High
Multiplex capability	No	No	Yes
Prognostic value	Low	Moderate	High

Note: Red text indicates optimal performance features.

Author Manuscript

Author Manuscript

Author Manuscript

Author Manuscript